

Probing the classical field approximation – thermodynamics and decaying vortices

Harry Schmidt^{1,2}, Krzysztof Góral¹, Filip Floegel^{1,3}, Mariusz Gajda⁴, and Kazimierz Rzążewski^{1,5}

¹ Center for Theoretical Physics, Polish Academy of Sciences, Aleja Lotników 32/46, 02-668 Warsaw, Poland

² Institut für Theoretische Physik I, Universität Stuttgart, Pfaffenwaldring 57, D-70550 Stuttgart, Germany

³ Institut für Theoretische Physik, Universität Hannover, D-30167 Hannover, Germany

⁴ Institute of Physics, Polish Academy of Sciences, Aleja Lotników 32/46, 02-668 Warsaw, Poland and

⁵ Cardinal Wyszyński University, Aleja Lotników 32/46, 02-668 Warsaw, Poland

We review our version of the classical field approximation to the dynamics of a finite temperature Bose gas. In the case of a periodic box potential, we investigate the role of the high momentum cut-off, essential in the method. In particular, we show that the cut-off going to infinity limit describes the particle number going to infinity with the scattering length going to zero. In this weak interaction limit, the relative population of the condensate tends to unity. We also show that the cross-over energy, at which the probability distribution of the condensate occupation changes its character, grows with a growing scattering length. In the more physical case of the condensate in the harmonic trap we investigate the dissipative dynamics of a vortex. We compare the decay time and the velocities of the vortex with the available analytic estimates.

I. INTRODUCTION

Experimental realization of Bose-Einstein condensation in a dilute gas of alkali atoms [1] stimulated a number of theoretical studies of the quantum degenerate, weakly interacting many body system. While the lowest energy state of the celebrated Gross-Pitaevski equation [2] describes remarkably well the properties of the condensate at zero temperature, the dynamics of the Bose gas at non-zero temperatures remains a challenge. The most successful description of the temperature dependence of the condensate oscillation frequencies and their damping rates has been obtained using different versions of the two gas models [3]. While useful, these models assume from the very beginning that the system at finite temperatures consists of two distinct factions: the condensate and the thermal cloud. A more fundamental approach would deduce the very existence of the condensed part directly from the dynamics of the many body system. In a series of papers, several groups [4, 5, 6, 7, 8] proposed a classical field approximation to fulfill this goal. In this approximation, the bosonic field operator is replaced by a classical field. This dramatic simplification is rooted in quantum electrodynamics, where classical electric and magnetic fields arise naturally if the number of quanta is large in a given mode. The classical field approximation is a simple and convenient technique describing the condensate in dynamical equilibrium with the thermal cloud, at temperatures close to the critical one. We have shown that the whole isolated system may be viewed as a single classical field undergoing nonlinear dynamics leading to a steady state [5, 8] (see also [6, 7]). The condensate is defined as the dominant term in the spectral decomposition of the time-averaged single-particle density matrix. Two cases were discussed: the box with periodic boundary conditions [5, 6, 7] and the realistic case of a spherically symmetric harmonic trap [8]. In our procedure it is the observation process and the finite detection time that allow for splitting the system into the condensate and the thermal cloud. The aim of the present paper is to further corroborate the details and the applicability of the classical fields approximation.

In Section II we briefly review the approximation based on

the classical fields. We stress again the need for the time averaging of the single particle density matrix for unambiguous splitting of the system into the condensed and uncondensed phases. The classical field approximation is introduced with the high momentum cut-off. In Section III we study in some detail the role of this cut-off in the model of a cubic box with the periodic boundary conditions. We also analyze the dependence of the cross-over energy on the value of the coupling constant. Within our approximation, it is a growing function of the scattering length. In Section IV, for the first time, we apply the method to a dynamical dissipative process. We phase imprint the vortex on a finite temperature, partially condensed Bose gas and track its decay. We conclude with the summary in Section V.

II. THE METHOD

We start with a brief description of our approach (some other details can be found also in [5, 6, 7, 8]). First, we consider the simplest case of a system of N bosonic atoms of mass m interacting via two-body forces. The N -body Hamiltonian written in the second quantization formalism has a form:

$$H = \int d^3r \hat{\Psi}^\dagger(\mathbf{r}) \frac{\mathbf{p}^2}{2m} \hat{\Psi}(\mathbf{r}) + \frac{g}{2} \int d^3r \hat{\Psi}^\dagger(\mathbf{r}) \hat{\Psi}^\dagger(\mathbf{r}) \hat{\Psi}(\mathbf{r}) \hat{\Psi}(\mathbf{r}), \quad (1)$$

where the first term is the kinetic energy and the second one is the energy of two-body interactions. In writing the Hamiltonian (1) we made a standard assumption: in the low energy limit a two-body interaction potential is approximated by a zero-range one. The interaction strength g is determined by a single parameter – the s-wave scattering length a_s , $g = 4\pi\hbar^2 a_s/m$. $\hat{\Psi}(\mathbf{r})$ is the field operator satisfying equal-time bosonic commutation relations:

$$[\hat{\Psi}(\mathbf{r}, t), \hat{\Psi}^\dagger(\mathbf{r}', t)] = \delta(\mathbf{r} - \mathbf{r}'). \quad (2)$$

The field operator can be expanded into any complete set of single-particle wave functions. One of these basis sets is of

particular importance – the one which corresponds to eigenfunctions of a single-particle density matrix[9]. This is because these functions have direct physical interpretation as they define coherent modes of the system. These modes are related to, typically performed, single-particle measurements. Note that a theoretical description of correlated measurements, which involve a simultaneous detection of a few particles, should be based on an appropriate multi-particle reduced density matrix. The single-particle mode of macroscopic occupation is a Bose condensate. In the ideal gas case eigenfunctions of the single-particle density matrix are obviously one particle states of the external potential. The situation becomes more complex if particles interact. In general, the eigenmodes are unknown. The only exception is a stationary system of particles trapped in a box with periodic boundary conditions. Here the symmetry of the problem imposes very strong constraints and eigenfunctions of the single-particle density matrix are simply plane waves – even in the presence of interactions. The field operator is therefore:

$$\hat{\Psi}(\mathbf{r}) = \sum_{\mathbf{k}} \frac{1}{\sqrt{V}} e^{-i\mathbf{k}\cdot\mathbf{r}} \hat{a}_{\mathbf{k}}, \quad (3)$$

where $a_{\mathbf{k}}$ is a bosonic operator which annihilates a particle of momentum \mathbf{k} . A full operator solution of the Heisenberg equation originating from the above Hamiltonian is not available and some approximations are necessary. Following Bogoliubov, at zero temperature, when all particles occupy a single zero-momentum mode, the corresponding annihilation operator can be substituted by a c-number amplitude, $\hat{a}_0 \rightarrow \sqrt{N}a_0$. This is possible because the commutator $[\hat{a}_0, \hat{a}_0^\dagger] = 1 \ll N$ is much smaller than the number of particles occupying the zero-momentum state. The remaining terms of the expansion (3) represent quantum corrections which in the lowest order of approximation are neglected. Let us note that the procedure leads to a substitution of the the full field operator by a c-number wave function:

$$\hat{\Psi}(\mathbf{r}) \rightarrow \sqrt{N}\Psi(\mathbf{r}). \quad (4)$$

The condensate wave function satisfies the Gross-Pitaevskii equation which is successfully used for description of low temperature behavior of the Bose-Einstein condensate:

$$i\hbar \frac{\partial \Psi(\mathbf{r}, t)}{\partial t} = \left(\frac{\mathbf{p}^2}{2m} + gN|\Psi(\mathbf{r}, t)|^2 \right) \Psi(\mathbf{r}, t). \quad (5)$$

This equation preserves both the energy and the particle number, i.e. the normalization of the wave function $1 = \int d^3r \Psi^*(\mathbf{r})\Psi(\mathbf{r})$. The Gross-Pitaevskii equation can also describe trapped condensates when a term describing the external potential is included.

Our approach is a simple generalization of the above procedure. Let us notice first that at relatively high energies (but below the critical one) there exists a number of modes, say M , whose occupation significantly exceeds unity, i.e. many different momentum states, up to a certain \mathbf{k}_{\max} are highly populated. Consequently, all corresponding annihilation operators

in the expansion (3) can be substituted by complex amplitudes and the remaining terms may be neglected:

$$\hat{\Psi}(\mathbf{r}) \rightarrow \sqrt{N} \sum_{\mathbf{k}}^{\mathbf{k}_{\max}} \sqrt{\frac{1}{V}} e^{-i\mathbf{k}\cdot\mathbf{r}} a_{\mathbf{k}} = \sqrt{N}\Psi(\mathbf{r}) \quad (6)$$

This approach evidently leads to the same Gross-Pitaevskii equation (5) for a wave function describing the “macroscopic part” of the whole system, or, more precisely, to its finite lattice version. This kind of approach is frequently used in quantum electrodynamics. The only difference from the zero temperature case is that now this wave function does not correspond to the minimal energy solution. Instead, it is a relatively high energy state. As it has been shown in[5, 6, 7], regardless of the particular choice of an initial state $\Psi(\mathbf{r}, t = 0)$, different than the Gross-Pitaevskii eigenstate, the system evolves towards the same stationary state uniquely determined by the energy and the particle number. More precisely, occupations of all macroscopically populated eigenmodes $N_{\mathbf{k}} = N|a_{\mathbf{k}}|^2$ fluctuate around their mean values[5]. The self consistency of the c-number approximation requires that all populations have to be large, $N_{\mathbf{k}} > 1$. To this end, the number of classical modes M has to be carefully chosen for each energy and particle number[6, 7]. This fact can be checked only *a posteriori* when the stationary populations are obtained. The intimate link between the energy, the number of particles and the number of modes is the essential ingredient of the whole method.

There is still one point which requires additional discussion. In fact, the “quasi-stationary” high energy solution of the Gross-Pitaevskii equation represents a pure state of the system with *all particles* in the same single state $\Psi(\mathbf{r}, t)$. Therefore, it seems to be totally unjustified to interpret $|a_{\mathbf{k}}|^2$ as relative occupations of different coherent modes of the system. The last concept is associated with a mixed state. Detailed inspection shows, however, that the relative phases of complex amplitudes $a_{\mathbf{k}}$ vary in time rapidly. On the other hand an observation process lasts for a finite period of time, typically of the order of hundreds of microseconds. It is sufficiently long for a “decoherence” of different eigenmodes:

$$\overline{a_{\mathbf{k}_1}^* a_{\mathbf{k}_2}} \equiv \frac{1}{\Delta t} \int_{t-\Delta t/2}^{t+\Delta t/2} d\tau a_{\mathbf{k}_1}^*(\tau) a_{\mathbf{k}_2}(\tau) \approx |a_{\mathbf{k}_1}|^2 \delta_{\mathbf{k}_1, \mathbf{k}_2}. \quad (7)$$

In the stationary regime the time averaged quantities do not depend on time. On the contrary, a temporal wave function of the whole system varies very rapidly. Therefore, what is being observed is related to a time averaged single-particle density matrix $\overline{\rho(\mathbf{r}_1, \mathbf{r}_2)} = \overline{\Psi^*(\mathbf{r}_1)\Psi(\mathbf{r}_2)}$. It is the observation that reduces a pure state to a mixed one. For particles trapped in a periodic box we have:

$$\overline{\rho(\mathbf{r}_1, \mathbf{r}_2)} = \frac{N}{V} \sum_{\mathbf{k}}^{\mathbf{k}_{\max}} e^{i\mathbf{k}(\mathbf{r}_1 - \mathbf{r}_2)} |a_{\mathbf{k}}|^2. \quad (8)$$

Eq.(8) shows that eigenvalues of the time averaged single-particle matrix are normalized occupations of different coherent modes of the system. We want to stress that the averaging

procedure is essential for the correct physical interpretation of the high energy solutions of the Gross-Pitaevskii equation. Note that instead of averaging over time, spatial averaging can be performed. Their importance can be fully appreciated in a more realistic case of harmonically trapped Bose condensates when eigenmodes of a single-particle matrix are not known. It is just diagonalization of the time averaged density matrix which gives simultaneously the eigenmodes and the populations. Results of our calculations for a harmonically trapped Bose condensate at finite energy are presented in[8]. The time averaged density has a characteristic bimodal pattern: sharp peak of condensed atoms embedded in a broad thermal cloud. On the other hand, an instantaneous distribution consists of a number of irregular spiky structures[8, 10]. According to our numerical calculations, the average width of a single spike is about three times larger than the healing length, the distance over which the condensate wave function heals back when perturbed locally. The characteristic length scale of the irregular structure is slightly larger (but of the same order) than the grid spacing necessary for description of the system of a given energy and particle number. As we have already mentioned, the self-consistency of the approximation requires a very precise selection of a number of modes M what in the present case directly translates into the grid spacing. In our approach M becomes an important, physical parameter.

III. BOSE-EINSTEIN CONDENSATE IN A PERIODIC BOX

In this section we explore our approach and present some important technical details. We consider here the system trapped in a periodic box because in this situation the coherent eigenmodes are uniquely determined by the symmetry of the potential. This greatly simplifies the problem. We numerically solve the Gross-Pitaevskii equation (5) on a finite grid using the Fast Fourier Transform split-operator method. The number of grid points is equal to the number of different momentum states. In order to explore the link between the number of macroscopically occupied modes, the number of particles and the energy we solve Eq.(5) in a 3D geometry varying the number of eigenmodes M only. In the calculations we keep the same initial state $\Psi(\mathbf{r}, t = 0)$ which guarantees that the energy per particle is constant. Similarly, the value of the following product is fixed:

$$gN = \text{const} \quad (9)$$

The results might seem surprising: the larger the number of modes M (with other parameters constant) the higher the occupation of the condensate mode $|a_0|^2 \rightarrow 1$.

This result requires a more detailed discussion. The total energy, the number of modes M and the product of gN are the *only* control parameters in our method. The number of particles N as well as the coupling strength g do not enter the dynamical equation (5) separately – it depends only on the product gN . Nevertheless, the condition of validity of the classical field approximation allows to determine the above parameters quite accurately. An occupation of the highest eigenmode

$N_{\mathbf{k}_{\max}} = N|a_{\mathbf{k}_{\max}}|^2$ must be larger than one. We arbitrarily set this value to 5. This way, having a stationary value of a relative occupation $|a_{\mathbf{k}_{\max}}|^2$, we can determine both N and g . It occurs that the requirement of self-consistency indicates that in our calculations the number of particles grows with M while the interaction strength g decreases in order to satisfy the condition (9). Only by examining the link between all parameters of the classical field approximation can we fully interpret our data.

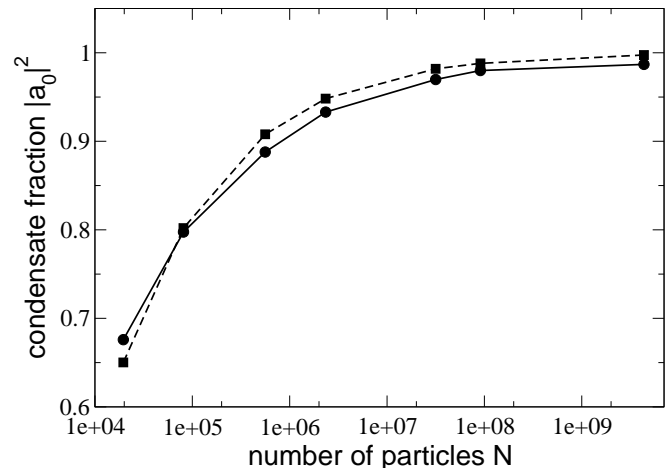


FIG. 1: Fraction of particles in the condensate $|a_0|^2$ as a function of particle number for $gN=\text{const}$. For comparison we show the curve given by the equation $|a_0|^2 = 1 - 8.2/N^{1/3}$.

In Fig.1 a relative abundance of the condensate atoms is plotted as a function of the number of particles. The condensate occupation can be quite accurately approximated by the following analytic expression:

$$|a_0|^2 \approx 1 - \frac{8.2}{N^{1/3}}. \quad (10)$$

This behavior is in agreement with a recent finding[11]. Lieb and Seiringer studied the properties of a true ground state N -body wavefunction of a system of N Bose particles interacting via two-body forces. They have shown that in the limit of $N \rightarrow \infty$ with $gN = \text{const}$ the relative population of the dominant eigenmode of the corresponding single particle density matrix approaches 1 while the eigenmode tends towards a ground state solution of the Gross-Pitaevskii equation. Our method shows how this limit is approached.

In the next series of calculations we estimate the interaction-induced shift of the cross-over energy for Bose-Einstein condensation. We prefer to use the term "cross-over energy" instead of "critical energy" as, strictly speaking, the critical energy is defined in the thermodynamic limit only. For a finite system (like the one we deal with here) several measures of the corresponding "cross-over" energy can be defined as there is no sharp phase transition. One of them [12] is based on the rapid change of the probability distribution of the condensate occupation.

We study the occupation of the condensate mode N_0 . The total energy of the system is changed while N and g are kept constant. This requires an optimization of the number of classical fields M to be taken into account: again, we set the occupation of the least occupied mode to 5 ($N_{k_{\max}} = 5$). The above constraint does not allow for a continuous change of the energy though. When a quasi-stationary state of a given energy is reached we trace a temporal population of the condensate mode $N_0(t)$ for a long time (about 10^5 time steps). This way we obtain a probability distribution of the condensate population which is presented in Fig.2. In this figure we show two characteristic distributions for different energies of the system. One of them (for the energy per particle $E = 43.8\hbar E_1$) is centered around some non-zero mean value of $N_0 \approx 5000$ (the grey histogram), while the other (for the energy $E = 49.5\hbar E_1$) is peaked at $N_0 = 0$. Here $E_1 = \hbar^2(2\pi)^2/(2mL^2)$ is the energy of the first excited state.

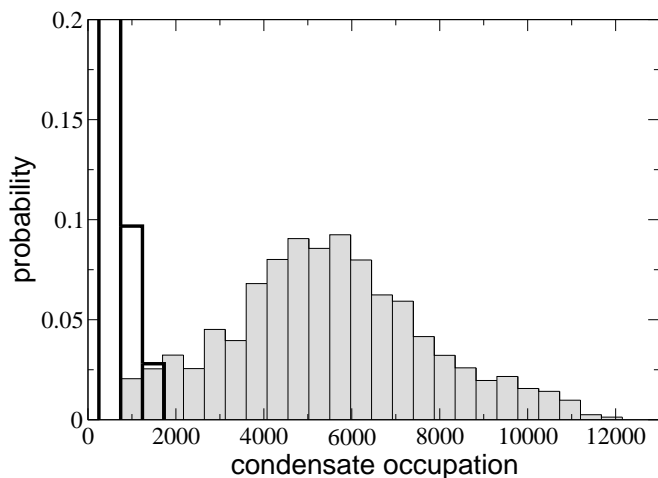


FIG. 2: Statistics of the condensate occupation in time. The grey histogram presents the case slightly below the cross-over energy (energy per particle $E = 43.8\hbar\omega$), while the transparent histogram corresponds to the situation above the cross-over energy (energy per particle $E = 49.5\hbar\omega$). Note that the highest bar of the latter histogram is off the scale of the figure (its value is 0.87). Here $N = 10^5$ and $g = 10^{-4}$.

Despite the fact that the values of energy for which both histograms are plotted are very similar, the rapid change of the character of the statistics evidently signifies the onset of Bose-Einstein condensation. The two energies give the lower and upper limit on the critical energy for a given interaction strength. We cannot determine the critical energy with better accuracy because of the previously discussed link between the parameters of our method. In the Fig.3 we show the upper and lower limits for the critical energy as a function of the coupling strength g . The critical energy grows with g . The same must happen to the critical temperature. We do not estimate the critical temperature as the method based on fitting the thermal distribution to the outer wings of the time averaged density profiles introduces a large uncertainty[8]. There is still a controversy in the literature[13] about the magnitude and the sign of the shift of critical temperature due to interac-

tions. The accuracy of our calculations, at the present stage, does not allow for a precise determination of this quantity. Nevertheless, they certainly indicate that the critical energy (and temperature) in the case of gas trapped in a box grows with interactions. The same conclusion for the classical field simulations in a box has been reached recently in [7].

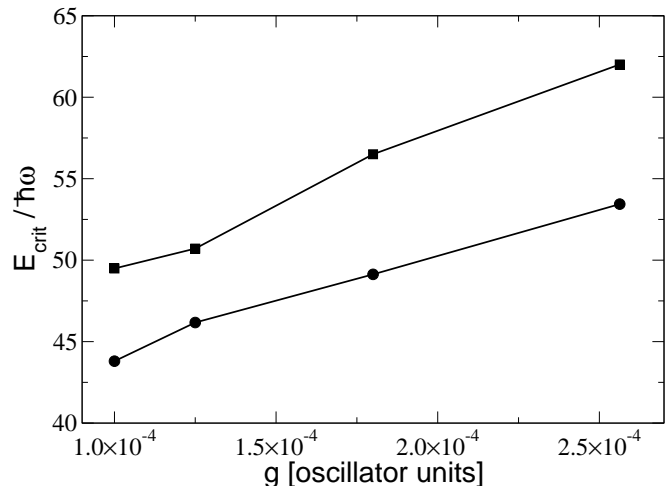


FIG. 3: Estimates of the critical energy of the phase transition based on the analysis of pairs of histograms like in Fig.2. Total number of particles is $N = 10^5$.

IV. VORTEX DYNAMICS AT FINITE TEMPERATURES

Creation of quantum vortices has provided a long-sought clear evidence of superfluidity in Bose-Einstein condensates of dilute atomic gases [14, 15]. Following the two pioneering experiments, various mechanisms of vortex nucleation have been investigated [16]. More recently, experiments have focused on peculiar properties of vortex lattices [17].

In most experiments vortices have been created in pure, essentially zero temperature, condensates. Very little has been said about finite temperature properties of these systems. Madison *et al.* [15], operating at temperatures below their detection limit, have measured finite vortex lifetimes of the order of 500-1000 ms. Anderson *et al.* [18] have seen no thermal damping on the time scale of 1 s. Finite temperature decay of vortex lattices has been also investigated [19]. Similarly, few theoretical works approached the problem. Fedichev and Shlyapnikov [20] show that it is the interaction of the thermal cloud with the vortex that provides a mechanism of energy dissipation. Due to that, an off-center vortex spirals out to the condensate boundary where it decays through the creation of excitations. For typical experimental parameters, they estimate the vortex lifetime to be in the range 0.1-10 s. Temperature dependence of the critical rotation frequency for the creation of vortices has been calculated in [21]. Bogoliubov as well as Hartree-Fock-Bogoliubov-Popov theories have been used to study the stability of vortex states at finite temperature

[22]. The role of filling the vortex core by the thermal cloud as a stabilizing factor has been emphasized [22].

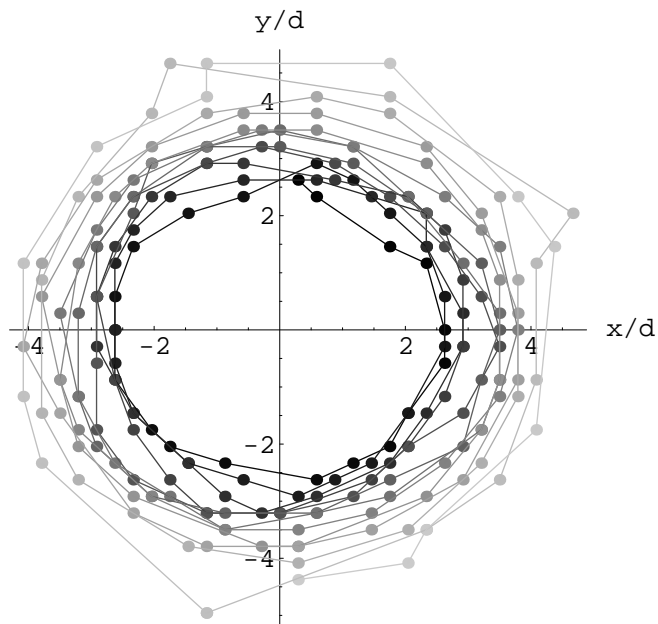


FIG. 4: Trajectory of a vortex core. The intensity of lines and dots fades away with time.

We have used the classical field method to study the dynamics of vortices in the presence of a thermal cloud. As an example, we consider 10^5 ^{87}Rb atoms in a spherically symmetric trap of frequency $\omega = 2\pi 100$ Hz. First, a suitable phase pattern (corresponding to a single quantum of circulation) is imprinted on a finite-temperature equilibrium state of an interacting Bose gas. Experimentally, phase imprinting is realized by shining a far off-resonant light on the condensate through a glass plate whose opacity varies continuously with an azimuthal angle. As a result, the condensate atoms acquire a phase depending on their location [23]. We situate the core of the vortex off the trap center. We see that the vortex created in this way starts moving around the trap center, slowly spiraling out to the border of the condensate. We follow the trajectory of the vortex core by time-averaging the gas density over short time. A sample trajectory of the vortex is shown in Fig.4. The equilibrium state used here for the phase imprinting contained about 48% atoms in the condensate (its energy being equal to $49.46 \hbar\omega$). The initial displacement of the vortex core from the trap center is $2.66d$. The Thomas-Fermi radius of a condensate consisting of 48000 ^{87}Rb atoms in our trap is $5.205d$ ($d = \sqrt{\hbar/m\omega} = 1.09\mu\text{m}$ being an oscillator unit of length) – note that the vortex disappears reaching roughly this distance from the trap center.

Fig.5 shows the time dependence of the distance of the vortex core from the trap center. One can see a slow drift towards the condensate boundary superposed on top of small fluctuations coming from the interaction with the thermal part of the system. From Fig.5 one can conclude that the radial velocity

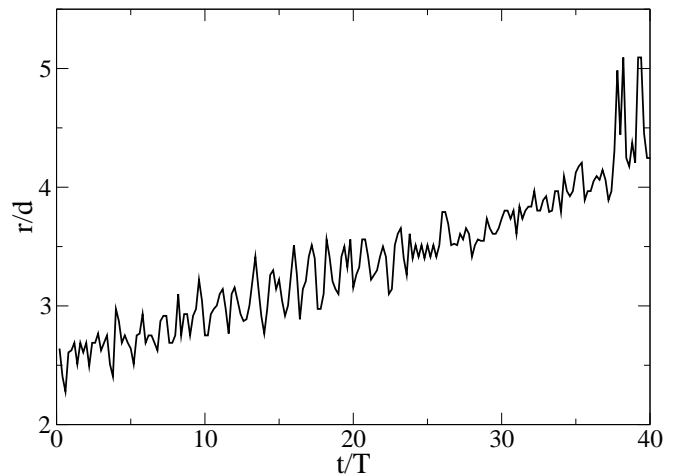


FIG. 5: Time dependence of the distance of the vortex core from the trap center. Time expressed in units of a trap period T .

of the vortex is roughly constant. Note also the vortex lifetime τ (here equal to about 37 trap periods).

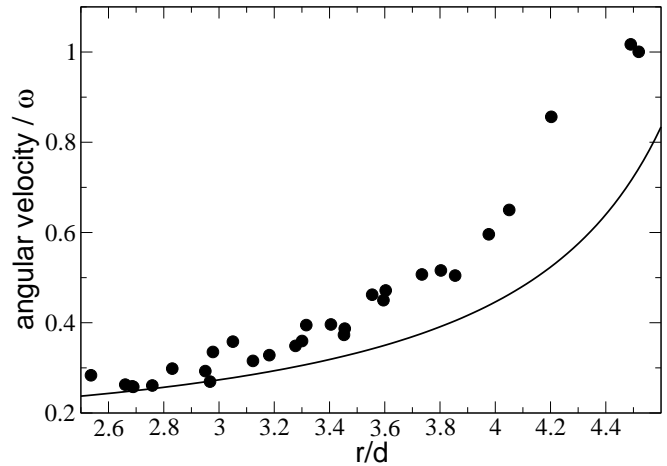


FIG. 6: Angular velocity of the vortex line (expressed in units of ω) as a function of its distance from the trap center. For comparison, an estimate of Fetter and Svidzinsky for a pure condensate of 48000 ^{87}Rb atoms in our trap is shown.

Fig.6 shows the angular velocity of the vortex core as a function of its (varying with time) distance from the trap center. One can see that the vortex moves faster and faster, in particular in the neighborhood of the condensate boundary. This result can be compared with theoretical predictions for pure, zero temperature, condensates – however, in this case there is no dissipation and off center singly quantized vortices in our case would follow *closed* circular trajectories. For pure condensates the angular velocity of the vortex line diverges at the condensate boundary [24]. We also see this kind of behavior in our data for a partly condensed Bose gas. To be specific, we have compared our data with a variational estimate provided by Eq.(87) in [24] (here $\Omega = 0$, as the trap is nonrotating) tak-

ing 48000 ^{87}Rb atoms. Despite notable differences between the two situations (presence or absence of dissipation due to the thermal cloud) the agreement is rather good even at the quantitative level.

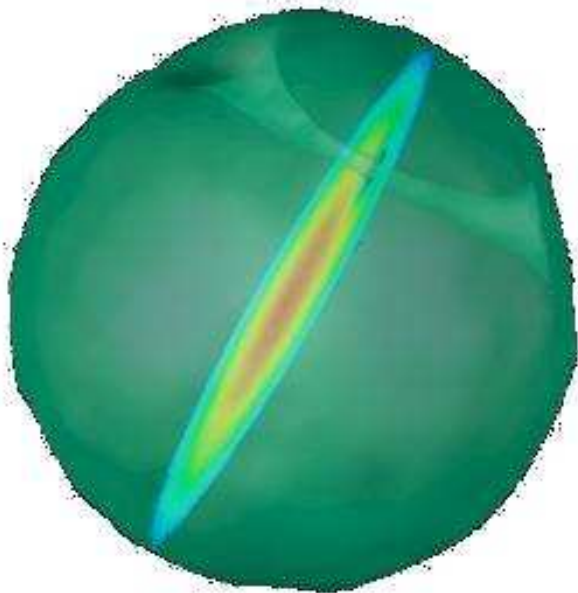


FIG. 7: 3-dimensional density of the gas cloud with a bent vortex line. The outer shell is a density isosurface near the condensate boundary. A plane with a surface density plot, perpendicular to the vortex line and through the trap center, is also shown.

More features of the vortex structure can be seen in Fig.7. In this figure a 3-dimensional density of the whole gas cloud, averaged over a short time, is depicted. The outer shell is an isosurface of density near the boundary of the condensate. The whole vortex line is visible in the upper part of the figure: one can see that it is bent at the edge of the condensate and it is much thicker there than in the center of the trap. The former observation agrees with recent experimental and theoretical results [25]. A plane perpendicular to the vortex line and through the trap center is also shown – it contains a surface density plot with a distinct hole at the vortex line.

So far we have kept the initial displacement of the vortex core fixed and simply studied the features of its trajectory. In the following, we look at the dependence of the vortex lifetime on its initial position in a trap. Fedichev and Shlyapnikov [20] calculate that:

$$\tau = \frac{m^2 R^2 \sqrt{\mu T}}{\hbar g \rho_n} \ln(R/x_{min}), \quad (11)$$

where R is the spatial size of the condensate (well approximated by the Thomas-Fermi radius), x_{min} is the initial displacement of the vortex line from the trap center, T is temperature and $\rho_n \approx 0.1 m^{5/2} T^{3/2} / \hbar^3$ is the mass density of the thermal cloud (for details of the derivation see [20]; however, note

the misprint in Eq.(12) of [20] – the bracketed factor should be raised to the power of $(-1/2)$ and not $(1/2)$ [26]).

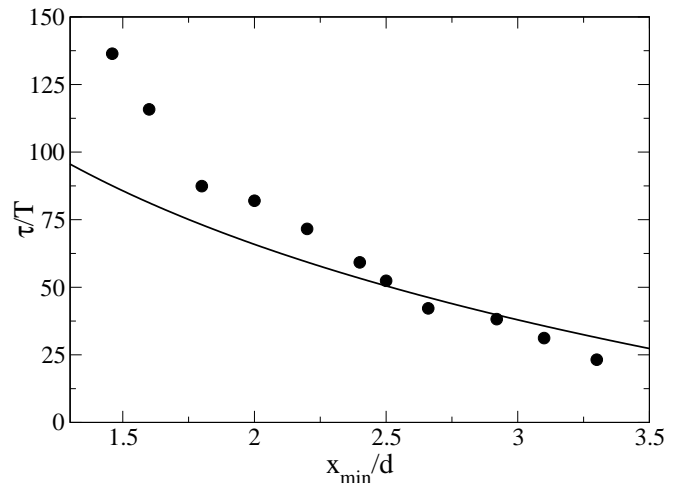


FIG. 8: Dependence of vortex lifetime τ on its initial displacement from the trap center x_{min} . Points come from our simulations while the solid line corresponds to Eq.(11).

In Fig.8 we plot the vortex lifetime as a function of its initial position (calculated from our simulations) as well as the values given by Eq.(11) (note that temperature of our system, for a given condensate fraction, has been estimated with the help of the ideal-gas formula with the finite-size corrections taken into account). One can see that it does agree quite well with the analytical estimate. However, one should note that one of the assumptions leading to the derivation of Eq.(11) is that the condition $T \gg \mu$ holds. In our case $T/\mu = 2.55$ which may be one of the reasons of the slight discrepancies between our data and the analytically predicted approximate values. Note that the total energy of the system is still fixed to $49.46 \hbar \omega$.

We have also investigated the variation of the vortex lifetime with the total energy (which amounts to its dependence on the condensate fraction). We have seen that this relation is much weaker than the one studied above. We have also noticed that even for a fixed initial displacement (which does not specify its position uniquely) the lifetime changes from shot to shot – in other words, the complex violent behavior of the thermal cloud in different regions of the trap makes the vortex lifetime a stochastic parameter.

V. CONCLUSIONS

We have reviewed our version of the classical field approximation to the dynamics of a finite temperature Bose gas. It provides an unambiguous splitting of the system into the condensed and uncondensed parts with the help of the time averaging of the single particle density matrix. In the case of a periodic box potential, we have investigated the role of the high momentum cut-off, essential in the method. In particular, we have shown that the cut-off going to infinity limit describes the particle number going to infinity with the scattering length

going to zero. In this weak interaction limit, the relative population of the condensate tends to unity. We have also shown that the cross-over energy, at which the probability distribution of the condensate occupation changes its character – one of several measures of the energies signifying the phase transition for the finite systems – grows with a growing scattering length. In the more physical case of the condensate in the harmonic trap we have investigated the dissipative dynamics of a vortex. We have compared the decay time and the velocities

of the vortex with the available analytic estimates.

The next step in going beyond the approximations employed in our model is the estimation of the influence of quantum corrections to the classical fields, in particular the study of the corresponding time scales.

We acknowledge support from the RTN Cold Quantum Gases. M.G. acknowledges support by the Polish KBN grant 2 PO3B 078 19. K.R. is supported by the subsidy of the Foundation for Polish Science.

-
- [1] M.H. Anderson, J.R. Ensher, M.R. Matthews, C.E. Wieman, and E.A. Cornell, *Science* **269**, 198 (1995); K.B. Davis, M.-O. Mewes, M.R. Andrews, N.J. van Druten, D.S. Durfee, D.M. Kurn, and W. Ketterle, *Phys. Rev. Lett.* **75**, 3969 (1995); C.C. Bradley, C.A. Sackett, J.J. Tollett, and R.G. Hulet, *ibid.* **75**, 1687 (1995) and Erratum **79**, 1170(E) (1997).
- [2] see, for example, F. Dalfovo, S. Giorgini, L.P. Pitaevskii, and S. Stringari, *Rev. Mod. Phys.* **71**, 463 (1999).
- [3] see, for example, B. Jackson and E. Zaremba, *Phys. Rev. Lett.* **88**, 180402 (2002).
- [4] B.V. Svistunov, *J. Moscow Phys. Soc.* **1**, 373 (1991); K. Damle, S.N. Majumdar, and S. Sachdev, *Phys. Rev. A* **54**, 5037 (1996); Yu. Kagan and B.V. Svistunov, *Phys. Rev. Lett.* **79**, 3331 (1997); N.G. Berloff and B.V. Svistunov, *Phys. Rev. A* **66**, 013603 (2002); K.Staliunas, cond-mat/0110258.
- [5] K. Góral, M. Gajda, and K. Rzążewski, *Opt. Exp.* **8**, 92 (2001).
- [6] M. J. Davis, S.A. Morgan, and K. Burnett, *Phys. Rev. Lett.* **87**, 160402 (2001); M.J. Davis, R.J. Ballagh, and K. Burnett, *J. Phys. B* **34**, 4487 (2001).
- [7] M.J. Davis, S.A. Morgan, and K. Burnett, cond-mat/020157.
- [8] K. Góral, M. Gajda, and K. Rzążewski, *Phys. Rev. A* **66**, 051602 (2002).
- [9] O. Penrose, *Phil. Mag.* **42**, 1373 (1951); O. Penrose and L. Onsager, *Phys. Rev.* **104**, 576 (1956); C.N. Yang, *Rev. Mod. Phys.* **34**, 694 (1962); for a recent discussion, see also A.J. Leggett, *Rev. Mod. Phys.* **73**, 307 (2001).
- [10] M. Gajda and K. Rzążewski, *Acta. Phys. Pol. A* **100**, 7 Suppl. S (2001).
- [11] E.H. Lieb and R. Seiringer, *Phys. Rev. Lett.* **88**, 170409 (2002).
- [12] M. Wilkens, F. Illuminati and M. Krämer, *J. Phys. B* **33**, L779 (2000).
- [13] K. Huang, *Phys. Rev. Lett.* **83**, 3770 (1999).
- [14] M.R. Matthews, B.P. Anderson, P.C. Haljan, D.S. Hall, C.E. Wieman, and E.A. Cornell, *Phys. Rev. Lett.* **83**, 2498 (1999).
- [15] K.W. Madison, F. Chevy, W. Wohlleben, and J. Dalibard, *Phys. Rev. Lett.* **84**, 806 (2000).
- [16] K.W. Madison, F. Chevy, V. Bretin, and J. Dalibard, *Phys. Rev. Lett.* **86**, 4443 (2001); C. Raman, J.R. Abo-Shaeer, J.M. Vogels, K. Xu, and W. Ketterle, *ibid.* **87**, 210402 (2001); P.C. Haljan, I. Coddington, P. Engels, and E.A. Cornell, *ibid.* **87**, 210403 (2001).
- [17] J.R. Abo-Shaeer, C. Raman, J.M. Vogels, and W. Ketterle, *Science* **292**, 476 (2001); P. Engels, I. Coddington, P.C. Haljan, and E.A. Cornell, *Phys. Rev. Lett.* **89**, 100403 (2002).
- [18] B.P. Anderson, P.C. Haljan, C.E. Wieman, and E.A. Cornell, *Phys. Rev. Lett.* **85**, 2857 (2000).
- [19] J.R. Abo-Shaeer, C. Raman, and W. Ketterle, *Phys. Rev. Lett.* **88**, 070409 (2002).
- [20] P.O. Fedichev and G.V. Shlyapnikov, *Phys. Rev. A* **60**, R1779 (1999).
- [21] S. Stringari, *Phys. Rev. Lett.* **82**, 4371 (1999).
- [22] S.M.M. Virtanen, T.P. Simula, and M.M. Salomaa, *J. Phys. C.: Condensed Matter* **13**, L819 (2001); S.M.M. Virtanen, T.P. Simula, and M.M. Salomaa, *Phys. Rev. Lett.* **86**, 2704 (2001); T. Mizushima, T. Isoshima, and K. Machida, *Phys. Rev. A* **64**, 043610 (2001).
- [23] Ł. Dobrek, M. Gajda, M. Lewenstein, K. Sengstock, G. Birkl, and W. Ertmer, *Phys. Rev. A* **60**, R3381 (1999).
- [24] A.L. Fetter and A.A. Svidzinsky, *J. Phys.: Condens. Matter* **13**, R135 (2001).
- [25] P. Rosenbusch, V. Bretin, and J. Dalibard, *Phys. Rev. Lett.* **89**, 200403 (2002); J.J. García-Ripoll and V.M. Pérez-García, *Phys. Rev. A* **64**, 053611 (2001).
- [26] G.V. Shlyapnikov, private communication.